Cell, Vol. 117, 337–347, April 30, 2004, Copyright ©2004 by Cell Press

Telomere Maintenance Requires the RAD51D Recombination/Repair Protein

Madalena Tarsounas,[1] Purificacíon Muñoz,[2] Andreas Claas,[1] Phillip G. Smiraldo,[3] Douglas L. Pittman,[3] María A. Blasco,[2] and Stephen C. West[1,*]

[1]Cancer Research UK
London Research Institute
Clare Hall Laboratories
Blanche Lane
South Mimms
Hertfordshire, EN6 3LD
United Kingdom

[2]Molecular Oncology Program
Spanish National Cancer Center
3 Melchor Fernandez Almagro
28029 Madrid
Spain

[3]Department of Physiology and Molecular Medicine
Medical College of Ohio
3035 Arlington Avenue
Toledo, Ohio 43614

Summary

The five RAD51 paralogs (RAD51B, RAD51C, RAD51D, XRCC2, and XRCC3) are required in mammalian cells for normal levels of genetic recombination and resistance to DNA-damaging agents. We report here that RAD51D is also involved in telomere maintenance. Using immunofluorescence labeling, electron microscopy, and chromatin immunoprecipitation assays, RAD51D was shown to localize to the telomeres of both meiotic and somatic cells. Telomerase-positive *Rad51d*$^{-/-}$ *Trp53*$^{-/-}$ primary mouse embryonic fibroblasts (MEFs) exhibited telomeric DNA repeat shortening compared to *Trp53*$^{-/-}$ or wild-type MEFs. Moreover, elevated levels of chromosomal aberrations were detected, including telomeric end-to-end fusions, a signature of telomere dysfunction. Inhibition of RAD51D synthesis in telomerase-negative immortalized human cells by siRNA also resulted in telomere erosion and chromosome fusion. We conclude that RAD51D plays a dual cellular role in both the repair of DNA double-strand breaks and telomere protection against attrition and fusion.

Introduction

Telomeres are large nucleoprotein complexes that protect the ends of chromosomes against degradation and fusion (Blackburn, 2001). Mammalian telomeric DNA consists of tandem repeats of a TTAGGG unit that extend for 10–15 kb in humans and end with a characteristic 3′ single-stranded DNA overhang on the G-rich strand. This 3′ overhang represents the substrate for extension by telomerase, a ribonucleoprotein that acts as a reverse transcriptase (McEachern et al., 2000). In the absence of telomerase, telomeres shorten progressively and lose their capping function (Blasco et al., 1997; Harley et al., 1990). Critically short telomeres or uncapped telomeres generate chromosome fusions that cause loss of replicative capacity, leading to senescence or apoptosis (Maser and DePinho, 2002).

A number of proteins that bind telomeric DNA with high sequence specificity and play a role in telomere protection have been characterized. TRF1 and TRF2 form multiprotein complexes that are required for chromosome capping (de Lange, 2002). These complexes regulate telomerase or facilitate its access to telomeric DNA. Additionally, TRF2 is thought to help protect telomeres by restructuring telomeric DNA into T loops in which the 3′ single strand invades the duplex region of the same telomere (Griffith et al., 1999; Muñoz-Jordan et al., 2001; Stansel et al., 2001; van Steensel et al., 1998). A telomeric single-strand overhang binding protein has also been identified, termed POT1, which regulates telomere elongation (Baumann and Cech, 2001; Baumann et al., 2002; Colgin et al., 2003; Loayza and de Lange, 2003).

Telomerase provides the major pathway for telomere elongation. However, it is thought that homologous recombination can provide alternative mechanisms for telomere length maintenance (ALT) and cell survival (Dunham et al., 2000; Henson et al., 2002; Le et al., 1999; Lundblad, 2002; Teng and Zakian, 1999). Consistent with this, telomerase-negative immortalized human cell lines contain subnuclear compartments, known as ALT-associated promyelocytic leukemia bodies (APBs), that include telomeric DNA, telomere-specific proteins, the recombination proteins RAD51 and RAD52, the MRE11/RAD50/NBS1 complex, the replication protein RPA, and the BLM and WRN DNA helicases (Henson et al., 2002). Approximately 10% of primary human tumors are thought to maintain telomere length in the absence of telomerase activity using the ALT pathway (Kim et al., 1994).

In mammalian cells, the RAD51 paralogs (RAD51B, RAD51C, RAD51D, XRCC2, and XRCC3) are involved in homologous recombination and are required for normal levels of resistance to DNA-damaging agents (Thacker, 1999). One member of this family, RAD51D, is essential for cell viability, as indicated by the embryonic lethality associated with disruption of the *Rad51d* gene in mouse (Pittman and Schimenti, 2000). Here, we demonstrate that RAD51D associates with telomeres and plays a dual cellular role, acting in double-strand break (DSB) repair and telomere maintenance. The involvement of RAD51D in telomere length regulation is independent of the telomerase activation status of cells.

Results

Telomeric Localization of RAD51D

The subcellular localization of RAD51D was examined in an asynchronous culture of telomerase-positive HeLa 1.2.11 cells, using a monoclonal antibody (mAb 5B3) raised against full-length human RAD51D. Although dif-

*Correspondence: stephen.west@cancer.org.uk

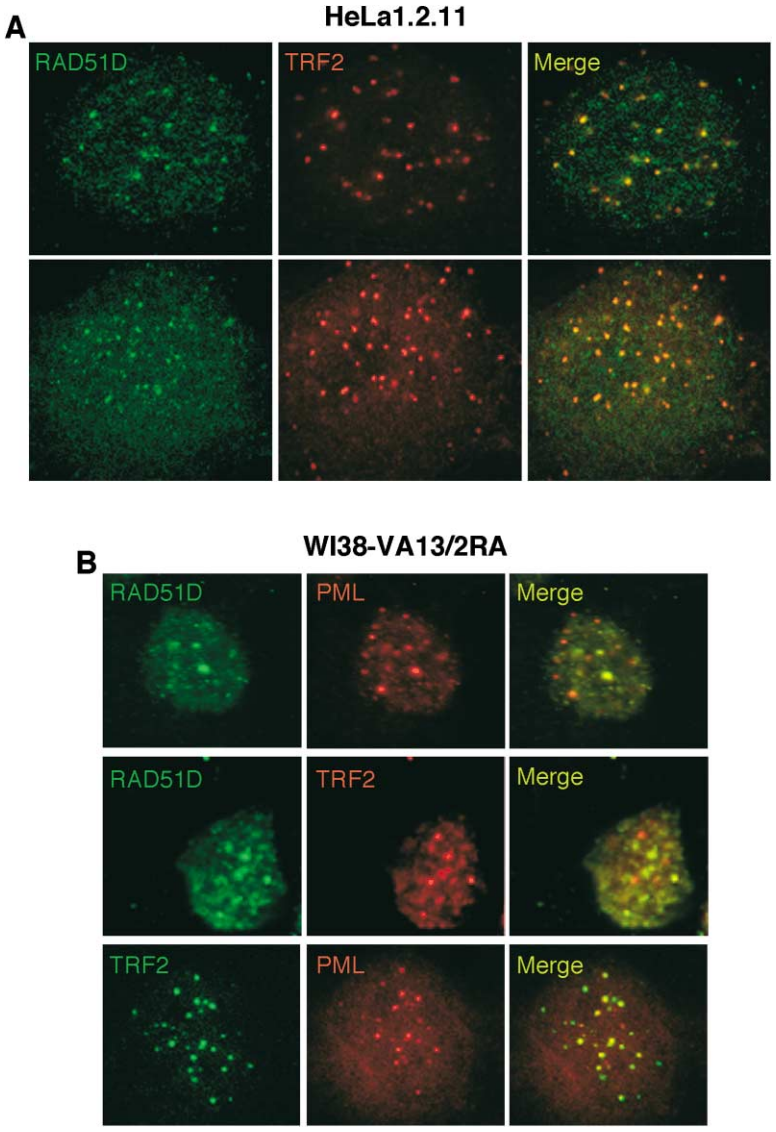

Figure 1. Localization of RAD51D in Telomerase-Positive and -Negative Somatic Cells

(A) Colocalization of RAD51D with TRF2 at HeLa telomeres. Nuclei were stained with anti-RAD51D mAb 5B3 (FITC, green) and anti-TRF2 pAb SWE38 (TRITC, red). Yellow foci in the merged images indicate colocalization.

(B) Human telomerase-negative WI38-VA13/2RA fibroblasts were stained with the following antibody combinations: anti-RAD51D pAbs SWE40 and anti-PML mAbs PG-M3 (top row), anti-RAD51D mAbs 5B3 and anti-TRF2 pAbs SWE38 (middle row), and anti-TRF2 pAbs SWE38 and anti-PML mAbs PG-M3 (lower row). RAD51D and TRF2 colocalize (yellow in merged images) to a subset of the PML bodies known as APBs.

fuse staining was seen throughout the nucleus, discrete nuclear foci were also observed (Figure 1A, green). Using dual indirect immunofluorescence with a number of proteins known to form nuclear foci either at S phase or in response to DNA-damaging agents (e.g., RAD51, RPA, BRCA1, BRCA2), the punctate pattern was found to be distinct from that characteristic of DNA repair foci. Instead, we found that RAD51D colocalized with TRF2, a protein that binds specifically to interphase telomeres (van Steensel et al., 1998) (Figure 1A). The telomeric localization of RAD51D was also seen in cells that were irradiated to promote DNA damage (data not shown). RAD51D was not observed in the radiation-induced RAD51 foci.

The telomeric localization of RAD51D in HeLa cells prompted us to examine RAD51D foci in telomerase-negative (ALT) cell lines, where several recombination proteins are known to colocalize with telomeres and telomere binding proteins to APBs, a subset of the promyelocytic leukemia (PML) bodies. As previously reported in human ALT cell lines (Henson et al., 2002), TRF2 localized to APBs identified with antibodies specific for PML. The data presented in Figure 1B show that RAD51D colocalized with TRF2 to the APBs. Taken together, the results presented in Figure 1 establish that RAD51D localizes to telomeres in both telomerase-positive and -negative somatic cells.

RAD51D Is Detected at the Telomeres of Meiotic Chromosomes throughout Prophase I

Meiotic telomeres have the advantage of being more easily visualized by immunofluorescence at the ends of paired chromosomes. We therefore prepared meiotic chromosome spreads from mouse spermatocytes and detected RAD51D while also visualizing the chromosome cores (axial elements) using an anti-SCP3 monoclonal antibody (Dobson et al., 1994) (Figure 2A). RAD51D was found to localize to all telomeres in these meiotic cells. We also observed that in the XY chromosome pair, which is only synapsed over a short region of homology known as the pseudoautosomal region, the RAD51D telomeric signal was detected both at the

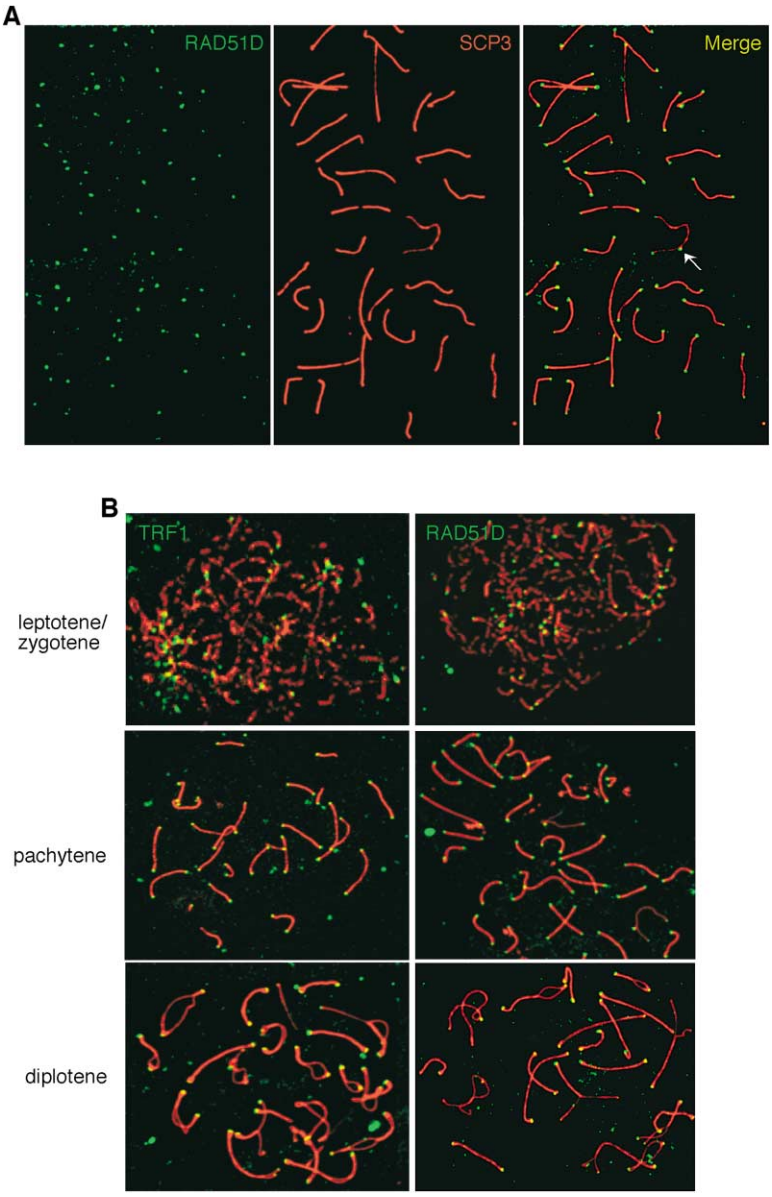

Figure 2. Colocalization of RAD51D with TRF1 at Meiotic Telomeres

(A) Mouse spermatocyte nuclei were immunostained with anti-RAD51D pAb SWE33 (green) and anti-SCP3 mAb 10G11 (red). The localization of RAD51D to chromosome termini is indicated in the merged image. The XY body is marked with an arrow.

(B) Spermatocyte nuclei at successive stages of meiotic prophase I were stained with anti-RAD51D pAb SWE33 (green) or anti-TRF1 pAb MTA17 (green) and anti-SCP3 mAb 10G11 (red).

synapsed end of the chromosome pair and at each individual end of the unpaired sex chromosomes (Figure 2A, arrow in merged image).

Next, the localization of RAD51D protein throughout meiotic prophase I was determined and compared with that of the telomere binding protein TRF1 (Chong et al., 1995; Scherthan et al., 2000). For this experiment, mouse spermatocytes were double stained using anti-RAD51D/anti-SCP3 or anti-TRF1/anti-SCP3. The initial stages of meiotic prophase I, leptotene/zygotene, were defined by a discontinuous SCP3 staining along the axial elements of unpaired chromosomes (Figure 2B). At this stage, the telomeres were seen to cluster together in a "bouquet" structure from which chromosome cores emerge. Groups of foci that identify bouquet formations were detected for both TRF1 and RAD51D. At pachytene, the axial cores synapsed fully to form the synaptonemal complex (SC), as identified by SCP3 staining. At this stage, and the following stage of diplotene when homologous chromosomes begin to separate, RAD51D and TRF1 were again visualized at the telomeres. These results show that RAD51D, like TRF1, localizes at the telomeres regardless of the synapsis status of the homologous chromosomes. When potential protein-protein interactions between RAD51D and TRF1/TRF2 were analyzed by coimmunoprecipitation from both testis and Hela extracts, and after coexpression using baculovirus-infected insect cells, we found no evidence to indicate direct interactions between these proteins.

In the experiments shown in Figures 1 and 2, RAD51D protein was detected using either mouse monoclonal or rabbit polyclonal antibodies raised against purified full-length protein. The specificity of the rabbit polyclonal antibody was confirmed by the loss of telomeric signal following its preincubation with purified RAD51D protein but not with RAD51 (data not shown). Similar immunofluoresence signals were observed when we used polyclonal sera raised in mouse against full-length

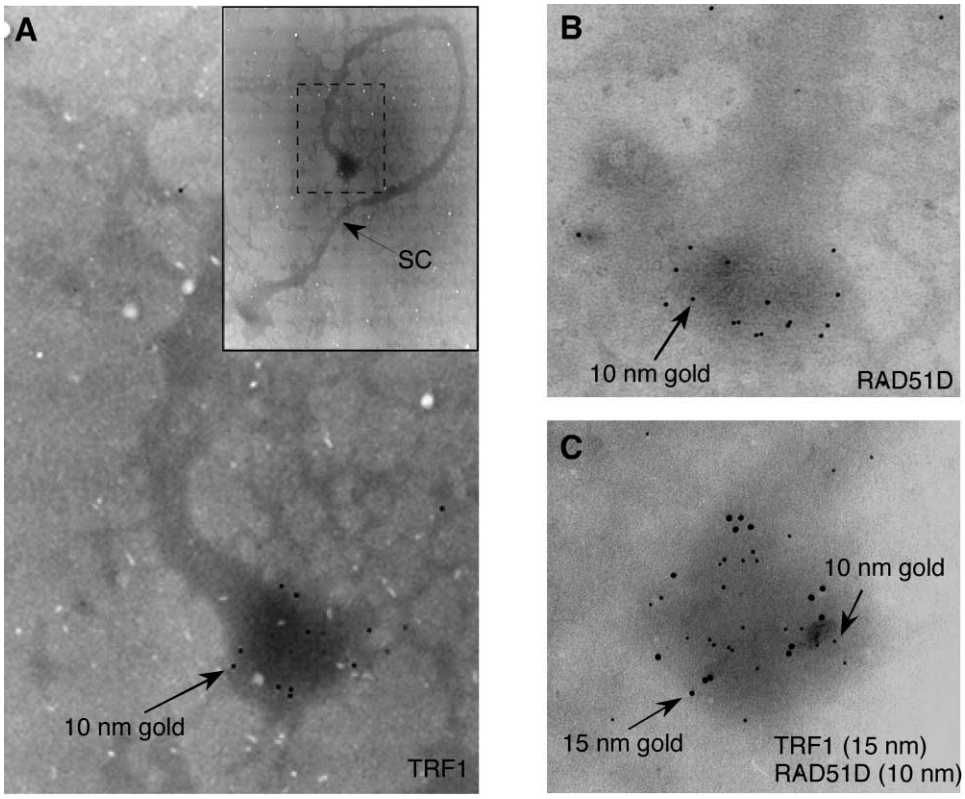

Figure 3. Electron Microscopic Visualization of RAD51D and TRF1 at Meiotic Telomeres by Immunogold Labeling

(A) Telomeric localization of TRF1 on a meiotic pachytene chromosome in which the telomere is seen as a bulky structure at the end of the synaptonemal complex (SC; see inset). TRF1 was visualized using a secondary antibody conjugated with 10 nm gold particles.

(B) Telomeric localization of RAD51D was carried out as described in (A) for TRF1.

(C) Colocalization of RAD51D and TRF1 at telomeres. In this case, the secondary antibodies against RAD51D and TRF1 were coupled to 10 and 15 nm gold particles, respectively.

RAD51D or against a synthetic peptide corresponding to residues 31–120 of RAD51D. No crossreaction against RAD51 or the other RAD51 paralogs has been observed by Western blotting or immunoprecipitation (data not shown).

The telomeric association of RAD51D was further analyzed at high resolution using immunogold labeling and electron microscopy. To do this, meiotic chromosome spreads were prepared from mouse spermatocytes and treated with DNase I to remove chromatin loops. Under these preparation conditions, the telomeres appear as bulky structures at the ends of the chromosome cores (Figure 3A, inset). The chromosome cores were then incubated with mouse anti-TRF1 mAb or rabbit anti-RAD51D pAb, either separately or together. TRF1 and RAD51D were subsequently detected using secondary antibodies conjugated with gold particles and visualized by electron microscopy (Figure 3). These single and dual labeling experiments provided further evidence for telomere binding by TRF1 and RAD51D.

ChIP Analysis of the Association of RAD51D with Telomeres

The association of RAD51D with telomeric DNA was confirmed by chromatin immunoprecipitation (ChIP) analyses performed with extracts prepared from either mouse testis (Figure 4) or asynchronous HeLa 1.2.11 cells (data not shown). The DNA and associated proteins in the extracts were crosslinked, fragmented by sonication, and then immunoprecipitated using various polyclonal antibodies. The presence of telomeric DNA was detected using ^{32}P-labeled probes corresponding to G-rich (Figure 4A) or complementary C-rich (Figure 4B) telomeric DNA strands. We found that the anti-RAD51D pAb pulled down RAD51D with associated telomeric DNA. In these experiments, the telomere-associated proteins TRF2 and RAP1 were used as positive controls. When a nontelomeric probe such as rDNA was used in the ChIP analysis, only the input extract generated a positive signal (Figure 4C). The data presented in Figures 4A and 4B are quantified in Figure 4D. In contrast to RAD51D, antibodies specific for other DNA repair proteins, such as RAD51, BRCA2, and the RAD51D-related paralogs RAD51C and XRCC2, gave telomeric ChIP signals at or below the level of the preimmune serum.

Telomere Dysfunction Induced by RAD51D Depletion in ALT Cells

To determine the role of RAD51D in telomere maintenance, we attempted to inhibit RAD51D synthesis in the telomerase-negative (ALT) human cell line WI38-VA13/2RA using siRNA technology. We found that transforma-

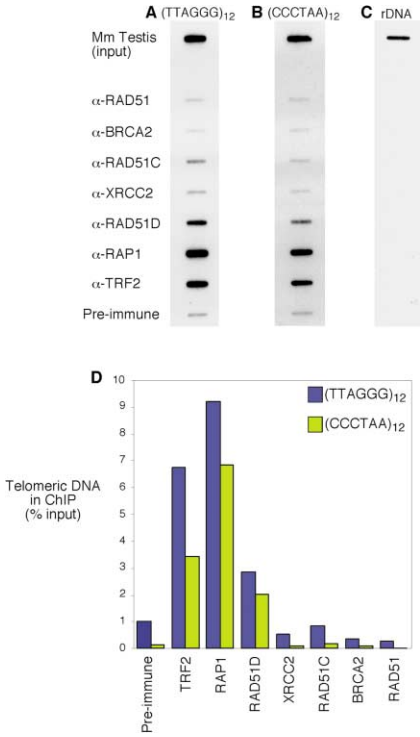

Figure 4. Telomeric Association of RAD51D Determined by Chromatin Immunoprecipitation

(A–C) ChIP analyses were carried out as described in Experimental Procedures using antibodies raised against RAD51 (FBE2), BRCA2 (SWE28), RAD51C (SWE31), XRCC2 (SWE35), RAD51D (SWE33), RAP1 (SWE39), and TRF2 (SWE38). Telomeric DNA was detected using ^{32}P-labeled G-rich (A) or C-rich (B) telomeric probes. An rDNA probe was used as negative control (C).

(D) Quantification of ChIP assays shown in (A) and (B) by phosphorimaging.

tion with two potential anti-RAD51D siRNA vectors (*51DsiRNA2* and *51DsiRNA3*) caused the majority of transfected cells to die within 7 days, whereas a different vector (*51DsiRNA1*) had little effect on cell growth (Figure 5A). Control experiments showed that *GFPsiRNA*, or vectors derived from one of the two inhibitory RNAs (*51DsiRNA2*) that contained two or four changes from the RAD51D sequence (*51DsiRNAmut1* or *2*), did not affect cell viability. When the kinetics of cell death were followed by determining the cell count after transfection with *51DsiRNA2* and the control *GFPsiRNA* construct, we found that at day 5, the *51DsiRNA2*-transfected cell population exhibited a 10-fold drop in viability. The loss of cell viability was associated with a 50% depletion of RAD51D protein, as determined by Western blotting (Figure 5B). The cell death accompanying RAD51D depletion was caused by apoptosis, as indicated by annexin V staining (data not shown). Based on these results and observations showing that inactivation of RAD51D in mouse cells leads to inviability (Pittman and Schimenti, 2000), we suggest that *51DsiRNA2* is an effective inhibitor of RAD51D synthesis.

We therefore examined whether depletion of RAD51D from the telomerase-negative cells affected telomere maintenance. To do this, we analyzed metaphase spreads of the surviving *51DsiRNA2*-transfected cells at day 5. An elevated frequency of end-to-end fusions was observed in the *51DsiRNA2*-transfected cells (1.2 fusions per metaphase; 64 events in 53 metaphases) compared to the *GFPsiRNA*-transfected control (0.5 fusions per metaphase; 31 events in 60 metaphases). Fusions involving two or more chromosomes were seen (Figure 5C). FISH analysis showed that fusions in which telomeric DNA was preserved at the site of the fusion occurred with a frequency of 1.0 fusions per metaphase in the *51DsiRNA2*-transfected cells, compared with 0.4 fusions per metaphase in the *GFPsiRNA*-transfected control cells ($p < 0.0001$).

When telomere length was measured using quantitative fluorescence in situ hybridization (Q-FISH) of metaphase nuclei using a telomere-specific probe (Figure 5D), we observed telomere shortening in the *RAD51D siRNA2*-transfected cells at day 5 compared with the *GFPsiRNA*-transfected cells ($p < 0.0001$). As shown in Figure 5E, there was an increase in the frequency of short telomeres (<6 kb) and a decrease in the frequency of longer telomeres (>20 kb). Calculated p values (<0.0001) for the two individual size groups shown in Figure 5E indicated that RAD51D depletion resulted in a statistically significant reduction in telomere length.

Telomere Attrition and Telomere-Related Chromosomal Abnormalities Induced by RAD51D Deficiency in MEFs

The data presented in Figure 5 indicate a defect in telomere maintenance following RAD51D inhibition. Any conclusions made from these experiments, however, must bear the caveat that the cells under analysis would soon become apoptotic, and it is known that apoptotic cells undergo telomere loss (Ramirez et al., 2003). We therefore analyzed telomere dysfunction in a cell line that is maintainable in culture. Although it has not been possible to establish *Rad51d*$^{-/-}$ knockout cell lines, recent studies have shown that the lethality associated with *Rad51d* mutation is delayed in a p53 mutant background (P.G. Smiraldo and D.L. Pittman, submitted). We therefore carried out Q-FISH analyses of telomeres in *Rad51d*$^{-/-}$ *Trp53*$^{-/-}$ primary mouse embryo fibroblasts and compared them with *Rad51d*$^{+/+}$ *Trp53*$^{-/-}$ and wild-type controls (Figure 6A). Two individually established MEFs were analyzed for each genotype, and a total of 3,656 (wild-type) and 4,044 (*Rad51d*$^{-/-}$ *Trp53*$^{-/-}$) individual telomere length measurements were obtained. We observed a significant decrease in telomere length, such that the average telomere length in *Rad51d*$^{+/+}$ *Trp53*$^{+/+}$ (49.3 kb) was reduced by more than 10 kb in *Rad51d*$^{-/-}$ *Trp53*$^{-/-}$ cells (38.9 kb). The *Rad51d*$^{+/+}$ *Trp53*$^{-/-}$ MEFs exhibited average telomere lengths similar to those found in the wild-type cells (49.2 kb), as described previously (Tong et al., 2001). We also found that there was a significant increase (from 3.53% to 11.5%) in the frequency of short telomeres (<20 kb) in the *Rad51d*$^{-/-}$ *Trp53*$^{-/-}$ MEFs in comparison with the control cells (Figure 6B). Correspondingly, the frequency of long telomeres (>60 kb) decreased from 23.7% to 12.6% in the double mutant versus wild-type MEFs.

We also examined whether the decrease in telomere length in the *Rad51d*$^{-/-}$ *Trp53*$^{-/-}$ MEFs was accompa-

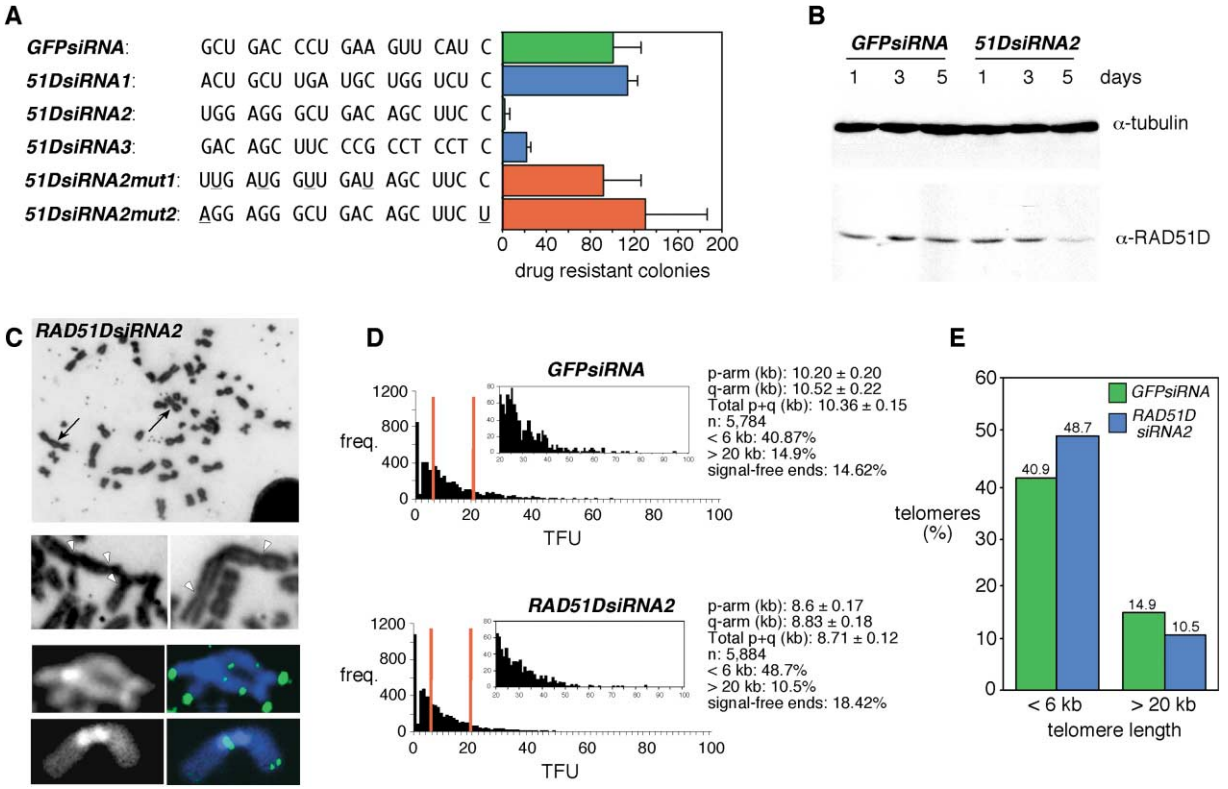

Figure 5. Cytological Analyses of WI38-VA13/2RA Cells Depleted of RAD51D by RNA Interference

(A) Cells were stably transfected with a control GFP siRNA or the indicated RAD51D siRNA constructs. At day 7, the number of surviving cell colonies was counted. Results are the mean of three independent experiments.

(B) Western blot analysis of extracts prepared from cells transfected with either *GFPsiRNA* or *RAD51DsiRNA2*. The same blot was probed with anti-RAD51D pAb or a mAb raised against tubulin (loading control).

(C) Cells at day 5 posttransfection were treated with demecolcine, and metaphase chromosomes were visualized by Giemsa staining. End-to-end fusions (arrows) and centromeres (white arrowheads) are indicated. Telomeric DNA was detected in RAD51D siRNA-treated ALT cells using FISH.

(D) Q-FISH analysis of telomere length distribution in cells transfected with RAD51D siRNA or GFP siRNA. The frequency of telomeres longer than 20 kb is indicated in the insets. TFU, telomere fluorescence units.

(E) Quantification of the relative changes in the frequency of short and long telomeres in cells transfected with either *GFPsiRNA* or *RAD51D siRNA2* (as indicated in [D]).

nied by a higher frequency of chromosome abnormalities. First, we found that the frequency of anaphase bridges, a fraction of which result from telomere dysfunction (de Lange, 2002; Goytisolo et al., 2001; Maser and DePinho, 2002), was increased 9-fold relative to the wild-type control (based on the analysis of 100 anaphases for each genotype, with two distinct cell lines per genotype). The anaphase bridge frequency observed in *Rad51d*$^{+/+}$ *Trp53*$^{-/-}$ cells was similar to that found in wild-type cells, as reported previously (Karlseder et al., 1999). Examples of normal (*Rad51d*$^{+/+}$ *Trp53*$^{+/+}$) and bridged (*Rad51d*$^{-/-}$ *Trp53*$^{-/-}$) anaphases as well as a representative bridged telophase from the mutant cell line are shown in Figure 6C. These results are similar to those observed previously in cell lines expressing a dominant-negative form of TRF2 (van Steensel et al., 1998). Immunofluorescence staining of *Rad51d*$^{+/+}$ *Trp53*$^{+/+}$ and *Rad51d*$^{-/-}$ *Trp53*$^{-/-}$ MEFs showed that the telomeric localization of TRF2 was normal in the *Rad51d*-deficient cells (Figure 6D).

Second, we observed and quantified a variety of chromosome aberrations (Figure 6E and Table 1). Three distinct types of events were scored: end-to-end fusions, chromosome lesions, and complex aberrations. End-to-end fusions were scored as events in which telomeric DNA sequences were either preserved or absent from the site of the fusion. The latter most likely arise from the religation of DSBs. We found a significant increase (2.5-fold) in spontaneous chromosomal lesions in the *Rad51d*$^{-/-}$ *Trp53*$^{-/-}$ MEFs, visualized as chromosome/chromatid breaks and fragments, when compared with the *Rad51d*$^{+/+}$ *Trp53*$^{-/-}$ MEFs. We also observed a large increase in the frequency of complex chromosomal aberrations (including tri- and quadriradials) in the *Rad51d*$^{-/-}$ *Trp53*$^{-/-}$ MEFs. Although these events were virtually absent in wild-type MEFs, they occurred at a frequency of 0.191 per metaphase in the *Rad51d*-deficient MEFs, most likely as a result of incomplete or illegitimate mitotic recombination events (Table 1, section A). Most importantly, we observed a 2.4-fold increase in the frequency of fusions that contained telomeric DNA at the fusion site when compared with the *Rad51d*$^{+/+}$ *Trp53*$^{-/-}$ MEFs ($p = 0.0025$; Table 1, section B). As end-to-end fusions containing telomeric sequences

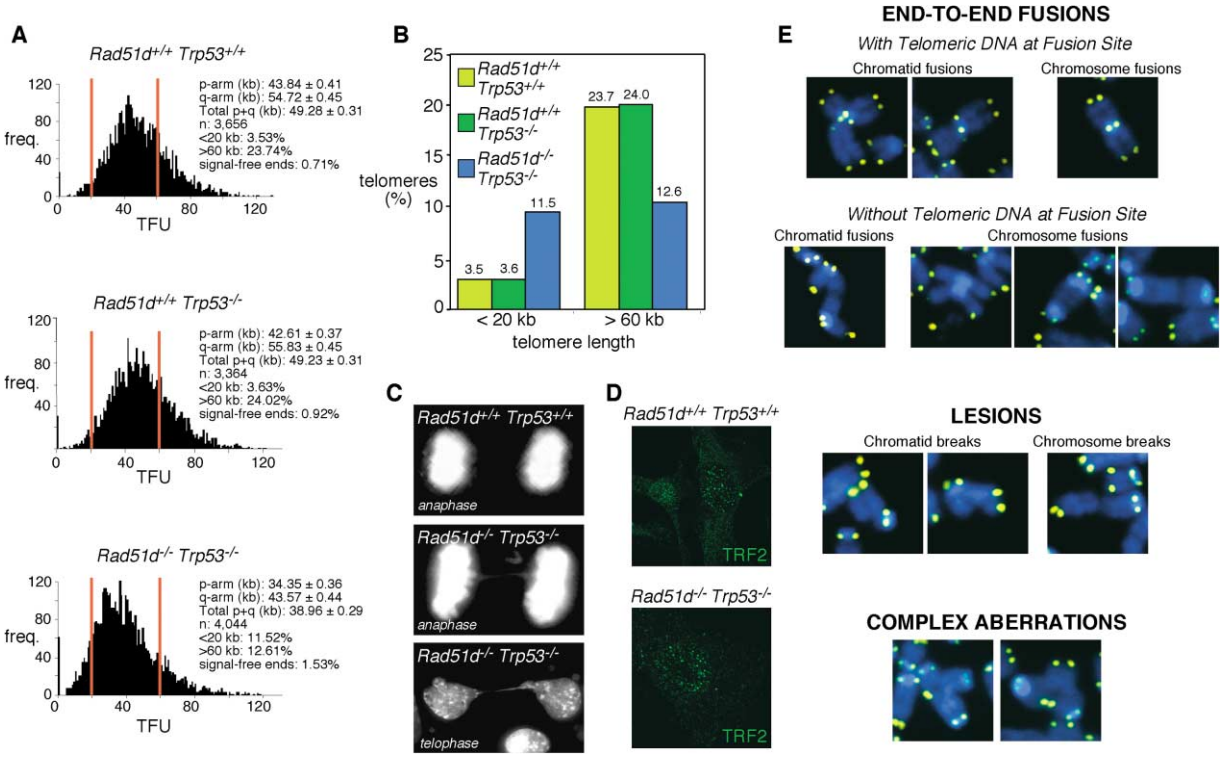

Figure 6. Telomere Dysfunction and Chromosomal Aberrations in *Rad51d*$^{-/-}$ *Trp53*$^{-/-}$ Primary MEFs

(A) Telomere length analysis by Q-FISH in *Rad51d*$^{+/+}$ *Trp53*$^{+/+}$, *Rad51d*$^{+/+}$ *Trp53*$^{-/-}$, and *Rad51d*$^{-/-}$ *Trp53*$^{-/-}$ MEFs. TFU, telomere fluorescence units. Two individually established cell lines were analyzed for each genotype.

(B) Quantification of the relative changes in the frequency of short and long telomeres in the three genotypes (as indicated in [A]).

(C) Anaphase and telophase bridges in the indicated primary MEFs.

(D) Immunofluorescence detection of TRF2 in the indicated primary MEFs using anti-TRF2 pAb SWE38.

(E) Metaphase chromosomes from *Rad51d*$^{-/-}$ *Trp53*$^{-/-}$-deficient cells were stained with DAPI, and the telomeres were visualized by FISH analysis. Examples of end-to-end fusions (with or without telomeric sequences at the fusion site) and a variety of chromosomal aberrations are shown.

are a characteristic signature of telomeric dysfunction (van Steensel et al., 1998), these results demonstrate that RAD51D is required for telomere maintenance.

Discussion

In this work, we have shown that the recombination/repair protein RAD51D interacts with mitotic and meiotic telomeres. Depletion of RAD51D in telomerase-negative cells or inactivation in telomerase-positive *Rad51d*$^{-/-}$ *Trp53*$^{-/-}$ MEFs led to the accumulation of telomeres with reduced length and resulted in a high incidence of telomeric end-to-end fusions. These telomere-specific events occurred in addition to the known defects in recombinational repair that cause a large increase in the frequency of chromosome/chromatid breaks and

Table 1. Cytological Analysis of Primary MEFs

(A) Frequency of Chromatid/Chromosome Breaks and Complex Aberrations in Primary MEFs of Indicated Genotypes as Determined by FISH

Parameter	*Rad51d*$^{+/+}$ *Trp53*$^{+/+}$	*Rad51d*$^{+/+}$ *Trp53*$^{-/-}$	*Rad51d*$^{-/-}$ *Trp53*$^{-/-}$
Number of metaphases	92	74	94
Complex aberrations[a]	0.000(0)	0.000(0)	0.191(18)
Chromatid/chromosome breaks[a]	0.109(10)	0.500(37)	1.245(117)

[a] Frequency of each aberration per metaphase. Examples of aberrations are illustrated in Figure 6. Two individually established cell lines were analyzed for each genotype, and the frequencies presented are mean values.

(B) Frequency of End-to-End Chromosome Fusions in Primary MEFs as Determined by FISH

Parameter	*Rad51d*$^{+/+}$ *Trp53*$^{+/+}$	*Rad51d*$^{+/+}$ *Trp53*$^{-/-}$	*Rad51d*$^{-/-}$ *Trp53*$^{-/-}$
Number of metaphases	162	132	149
Total end-to-end fusions[b]	0.043(7)	0.235(31)	0.570(85)
−TTAGGG[b]	0.012(2)	0.136(18)	0.336(50)
+TTAGGG[b]	0.031(5)	0.098(13)	0.234(35)

[b] Frequency of each aberration per metaphase. The number of events for each type of aberration is shown in parentheses. +TTAGGG and −TTAGGG refer to the presence or absence of telomeric repeats at the fusion point, respectively. Two individually established cell lines were analyzed for each genotype, and the frequencies presented are mean values.

fusions resulting from nonhomologous end-joining processes. While a number of proteins involved in DNA repair, including MRE11/RAD50/NBS1 complex (Zhu et al., 2000), Ku70/80 (Bianchi and de Lange, 1999; Espejel et al., 2002; Hsu et al., 1999, 2000; Samper et al., 2000), ERCC1/XPF (Zhu et al., 2003), RAD54 (Jaco et al., 2003), and DNA-PK_{cs} (Bailey et al., 1999; Gilley et al., 2001; Goytisolo et al., 2001), are known to be required for telomere maintenance, to our knowledge, this study provides the first direct visualization of the stable association of a homologous recombination/repair protein with mammalian telomeres.

Dual Role for RAD51D Protein in DSB Repair and Telomere Protection

Previous studies of the cellular defects associated with *RAD51D* mutation were restricted to chicken DT40 cell lines (Takata et al., 2001), because disruption of *Rad51d* in rodent cells resulted in inviability (Pittman and Schimenti, 2000). Inactivation of *rad51d* in DT40 led to high levels of spontaneous cell death, and those cells that remained viable accumulated chromosomal aberrations and were hypersensitive to DNA-damaging agents. The cells were also defective in targeted integration and sister chromatid exchange. These phenotypes are consistent with the involvement of RAD51D in recombinational repair (Takata et al., 2001). Similar characteristics were exhibited by DT40 cell lines disrupted in each of the other four *rad51* paralogs: *rad51b*, *rad51c*, *xrcc2*, and *xrcc3*. However, in comparison with the other paralogs, *rad51d* mutant cells exhibited a significant increase in the number of spontaneous chromosome breaks, raising the possibility of a more severe genomic instability defect in this mutant and a unique role for RAD51D in chromosome metabolism.

The observation that RAD51D localized to the telomeres of meiotic and somatic chromosomes as well as its association with telomeric DNA in ChIP assays led us to determine whether RAD51D played a role in telomere maintenance. In a telomerase-negative immortalized human cell line, RAD51D and TRF2 colocalization was observed in APBs. In addition to telomeric DNA and telomere-specific proteins, APBs contain the recombination proteins RAD51 and RAD52, the MRE11/RAD50/NBS1 complex, the replication protein RPA, and the BLM and WRN proteins (Henson et al., 2002) and are thought to represent sites of telomere regeneration. We also found RAD51D at meiotic telomeres, where it colocalized with the telomeric marker TRF1 throughout prophase I. We did not observe the association of RAD51D along paired chromosomes, as seen previously with RAD51 (Barlow et al., 1997; Moens et al., 1997; Scully et al., 1997). However, the limitations of immunofluorescence localization do not eliminate the possibility that RAD51D may play an important role in the repair of meiotic DSBs. Indeed, we expect that RAD51D will be involved in meiotic recombination, but such analyses are not possible at this time, due to the lack of a *Rad51d*-defective mouse.

Mice homozygous for *Rad51d* deletion show early embryonic lethality between 8.5 and 11.5 days (Pittman and Schimenti, 2000). Additionally, it has not been possible to generate *Rad51d*$^{-/-}$ MEFs or ES cell lines. However, while embryonal survival is only slightly prolonged in a p53 null background to day 16.5, MEFs deficient for both *Rad51d* and *Trp53* have been maintained in culture (P.G. Smiraldo and D.L. Pittman, submitted). Analysis of the MEFs revealed a strikingly high incidence of chromosomal aberrations, including chromatid and chromosomal breaks and dicentric chromosomes. Similar chromosomal aberrations have been described in cell lines lacking proteins involved in recombinational repair and replication fork maintenance, such as BRCA2 (Venkitaraman, 2002), Bloom's syndrome (German, 1993), ataxia telangiectasia (Khanna and Jackson, 2001), and Fanconi's anemia (D'Andrea and Grompe, 2003). In all these cell lines, chromosomal aberrations arise spontaneously in the absence of DNA damage, indicating that they originate during DNA replication when stalled or broken replication forks fail to be repaired normally.

In addition to this replication-associated DNA repair defect, we found that both mouse and human cell lines lacking RAD51D showed a statistically significant increase in the number of end-to-end fusions involving dysfunctional telomeres, as indicated by the presence of telomeric repeats at the site of the fusion. High levels of end-to-end fusions have been reported in cells overexpressing a dominant-negative version of TRF2, which interferes with the binding of wild-type TRF2 to the telomeres (van Steensel et al., 1998). Our results indicate that the end-to-end fusions, detected as a consequence of the *Rad51d* deletion, occur independently of TRF2, as immunofluorescence studies have shown that the telomeric localization of TRF2 was unaffected in the *Rad51d*$^{-/-}$ *Trp53*$^{-/-}$ cells. At this time, however, we cannot exclude the possibility that RAD51D inactivation results in the dissociation of other essential telomere binding factors.

A Recombination-Mediated Pathway for Telomere Maintenance

Given the two aspects of chromosomal stability that require RAD51D (DNA repair and telomere maintenance), it is possible that the severe genomic instability observed in the *Rad51d*-defective cells could be due to an additive effect of a replication-associated repair defect and a localized instability generated by unprotected telomeres. Quantitative FISH analyses showed significant telomere shortening in both the RAD51D siRNA-depleted telomerase-negative cells and, in particular, the telomerase-positive *Rad51d*$^{-/-}$ *Trp53*$^{-/-}$ MEFs.

The average telomere shortening observed in primary *Rad51d*$^{-/-}$ *Trp53*$^{-/-}$ MEFs was approximately 21% (from an average telomere length of 49 to 39 kb) and is comparable to the 32% loss of telomeric sequences in *Rad54*$^{-/-}$ MEFs (from 43 to 29 kb) (Jaco et al., 2003). Similar levels of telomere shortening have been observed with MEFs from telomerase-deficient mice (Blasco et al., 1997). Assuming that RAD51D and RAD54 act in the same pathway for recombination-mediated telomere maintenance, these data indicate that recombination functions and telomerase are both required for normal telomere homeostasis. However, the high incidence of end-to-end fusions involving telomeric repeats observed in the *Rad51d*-deficient MEFs leads us to suggest a role for RAD51D in telomere capping. The attrition phenotype may be due to a loss of capping functions that render

the telomere prone to nucleolytic degradation (Ferreira et al., 2004).

Our results demonstrate the constitutive presence of a recombination protein at telomeres. It remains to be established whether recombination is required for telomere elongation, by strand invasion followed by template directed DNA synthesis, or for protection of the telomeric single-strand overhang. We favor the hypothesis that the mechanism of telomere maintenance requiring RAD51D involves telomere capping, such that loss of RAD51D would lead to loss of protection and subsequent telomere attrition. Critically short telomeres would then be subjected to end-to-end ligation reactions leading to the observed chromosome fusions. Alternatively, short telomeres may be fused to nontelomeric DNA ends that occur at sites of collapsed replication forks.

It has been proposed that telomeric ssDNA overhangs may be protected by ssDNA binding proteins, telomere-specific end binding proteins such as POT1 (Baumann and Cech, 2001; Baumann et al., 2002; Colgin et al., 2003; Loayza and de Lange, 2003), or the formation of T loop structures by invasion of the 3′ ssDNA overhang into internal duplex telomeric repeats (de Lange, 2002; Griffith et al., 1999). T loops are thought to be similar in structure to D loops that form at the initial strand invasion step of homologous recombination and can be processed into Holliday junction-like structures by branch migration of the loop. Recently, two of the five RAD51 paralogs were implicated in Holliday junction processing reactions, as *RAD51C*- and *XRCC3*-defective hamster cell lines were shown to contain reduced levels of Holliday junction resolvase activity (Liu et al., 2004). In vitro data also support the concept that other members of the RAD51 paralog family of proteins act at Holliday structures: (1) RAD51B was shown to bind specifically to Holliday junctions (Yokoyama et al., 2003), (2) the RAD51B-RAD51C-RAD51D-XRCC2 complex has been implicated in branch migration (Liu et al., 2004), and (3) purified RAD51D-XRCC2 interacts with BLM and stimulates its actions at Holliday junctions (Braybrooke et al., 2003). It may also be significant that BLM localizes to telomeres and interacts with TRF2 (Opresko et al., 2002; Stavropoulos et al., 2002).

Currently, RAD51D appears to be unique among the RAD51 paralogs in its ability to interact constitutively with telomeres. However, our work does not exclude weak or transient telomere binding by other members of this protein family, leading to assembly of Holliday junction processing complexes. These would be expected to provide a junction protection or capping function, since the nuclease functions of the mammalian resolvase are, like those of bacterial RuvC, dependent upon preferred sequences that may not be present within repetitive telomeric DNA (Constantinou et al., 2001). We therefore propose that RAD51D protein may play a dual role in both the recombinational repair of DSBs and telomere protection by stabilization of T loop or Holliday junction-like intermediates present at the ends of mammalian chromosomes.

Experimental Procedures

Antibodies

Rabbit polyclonal antibodies (pAbs) against human RAD51C (SWE31), RAD51D (SWE33), XRCC2 (SWE35), RAD51 (FBE2), BRCA2 (SWE28), and the RAD51D monoclonal antibody (mAb; 5B3) are described elsewhere (Davies et al., 2001; Masson et al., 2001; Tarsounas et al., 2003). Rabbit pAb SWE40 was raised against a peptide comprising residues 31–120 of human RAD51D. Mouse anti-TRF1 (MTA17), rabbit anti-TRF2 (SWE38), and rabbit anti-RAP1 (SWE39) pAbs were raised against purified human TRF1, TRF2, and RAP1 proteins. Mouse mAb anti-SCP3 (10G11) was made using purified hamster SCP3 protein. The anti-PML mAb (PG-M3) was purchased from Santa Cruz Biotech. For Western blotting, we used a rabbit anti-RAD51D pAb IH42 raised against amino acids 120–328 of the protein (Braybrooke et al., 2000) and an anti-α-tubulin mAb (TAT-1; Cancer Research UK).

Immunofluorescence Staining

HeLa 1.2.11 cells (van Steensel et al., 1998) were grown on coverslips and immunolabeled as described (Tarsounas et al., 2003), except that an additional fixation step in cold methanol (10 min at -20°C) was carried out before blocking. PML bodies were visualized in a similar way in WI38-VA13/2RA cells (Bryan et al., 1995), except that the hypotonic treatment was replaced by a preextraction step performed in 20 mM HEPES (pH 7.5), 0.25% Triton X-100, 50 mM NaCl, 3 mM $MgCl_2$. Spermatocytes from 6-week-old mice were spread on the surface of hypotonic solution and antibody stained as described (Dobson et al., 1994), except that the samples were fixed in 4% paraformaldehyde prior to treatment with 4% paraformaldehyde/0.02% SDS. Specimens were viewed on a Zeiss laser scanning confocal microscope, LSM 510. In experiments in which two proteins were examined for colocalization, controls were carried out to make sure there was no bleed through from the red to the green channel. For this, single-staining experiments were performed in which one of the primary antibodies was omitted, whereas both secondary antibodies were applied as usual.

Electron Microscopy

Spermatocyte spreads were prepared as described (Dobson et al., 1994), except that the OsO_4 step was omitted. Secondary antibodies coupled to 10 or 15 nm gold particles were obtained from British BioCell International. Samples were visualized using a Jeol EM1010 electron microscope at 12,000$\times$ magnification.

Chromatin Immunoprecipitation Assays

Testicular cells were obtained from six mouse males less than 6 months old. Suspensions were prepared essentially as described (Tarsounas et al., 1999), and cells were lysed in 5 ml fractionation buffer (10 mM HEPES, 5 mM KCl, 1.5 mM $MgCl_2$, 0.5% NP-40) with protease inhibitors and held on ice for 10 min. Following centrifugation, nuclei were treated with 4% paraformaldehyde in PBS. SDS (0.1%) was then added, and fixation continued for 5 min. The nuclei were pelleted, washed two times in PBS, and resuspended in ChIP buffer (50 mM Tris-HCl [pH 7.5], 2 mM EDTA, 1% NP-40) containing 0.2 M NaCl. After 10 min on ice, the DNA was sheared by sonication to generate fragments between 0.1 and 1.0 kb. The extract was cleared by centrifugation, and protein-DNA complexes were pulled down by incubation with primary antibody crosslinked to Aminolink beads (Pierce) at 4°C for 12 hr. The beads were washed four times in ChIP buffer containing 0.5 M NaCl, and protein-DNA complexes were eluted in 50 mM Tris-HCl (pH 8.0), 10 mM EDTA, 1% SDS. To reverse crosslinking, the complexes were incubated overnight at 65°C, and proteins were removed by treatment with proteinase K. The DNA was purified and denatured at 65°C in 0.4 M NaOH and then slot blotted into a Hybond C+ membrane. The membrane was washed in 0.5 M Tris-HCl (pH 8.0), 0.15 M NaCl, air dried, blocked, and hybridized with 5′ ^{32}P-labeled G strand $(TTAGGG)_{12}$ and C strand $A(CCCTAA)_{12}$ probes overnight at 65°C.

siRNA

Telomerase-negative WI38-VA13/2RA cells were grown to 70% confluence and transfected with pSUPER.retro (OligoEngine) siRNA constructs (Brummelkamp et al., 2002). After 48 hr, transfected cells were selected using 1.0 μg/ml puromycin. Colony formation was examined at day 7 posttransfection. Media was removed from the plates, and cells were washed in PBS, stained in Leishman's solution for 5–10 min, and washed with distilled water for 5 min. Colonies larger than 1 mm in diameter were counted. To determine cell

counts, cells were trypsinized and counted every day for 7 days after transfection. Transfection efficiencies were monitored by GFP expression from a control vector and found to be similar for each siRNA construct.

To analyze RAD51D expression in siRNA-treated cells, cell pellets were washed in PBS, resuspended in four times pellet volume of lysis buffer (50 mM Tris [pH 8.0], 0.5 M NaCl, 0.4% NP-40, 10% glycerol), and extracted on ice for 30 min. The extract was then sonicated and cleared by centrifugation at maximum speed on a bench-top centrifuge. Volumes corresponding to equal numbers of cells (1×10^6) were analyzed by Western blotting. The anti-tubulin antibody was used as a loading control.

Chromosome Analyses

Five days after transfection with siRNA vectors, the WI38-VA13 cells were treated with 0.1 μg/ml demecolcine for 90 min, harvested by trypsinization, incubated for 15 min at room temperature in 50 mM KCl, 1% Na citrate, and fixed in a freshly prepared 3:1 mix of methanol:glacial acetic acid. Nuclear preparations were stored at −20°C, and chromosomes were spread on slides that were prewarmed to 60°C. One hundred Giemsa-stained metaphases were examined for each cell sample. One fusion event was defined as the result of joining of two or more chromosomes. The end-to-end fusion index was calculated as the number of events per total number of metaphases. Fluorescence in situ hybridization (FISH) was performed according to standard techniques using 15 ng/μl FITC-conjugated PNA $[CCCTAA]_3$ telomeric probe (Applied Biosystems), and chromosomes were visualized with DAPI.

Primary MEFs isolated from matings between mice heterozygous for *Rad51d* and *Trp53* or just *Trp53* (Jacks et al., 1994; Pittman and Schimenti, 2000) were passaged once and either seeded onto glass coverslips and stained with DAPI or treated with 0.1 mg/ml demecolcine for 90 min, trypsinized, and fixed as above for metaphase spreads. Fifty anaphases per cell line from two independent cell samples of each genotype were scored. Anaphase bridging was defined as anaphases in which the bridging chromosomes spanned the entire distance separating the anaphase poles.

FISH hybridization was performed according to a protocol from PerkinElmer. Q-FISH analyses were performed as indicated (Herrera et al., 1999), and statistical analyses of chromosomal aberrations were carried out as described (Jaco et al., 2003). The Q-FISH data presented in Figures 5D and 6A were subjected to statistical analyses using Wilcoxon's rank sum test (Hemann et al., 2001). The p values relating to the two individual size groups shown in Figure 5E were determined by a chi-square test.

Acknowledgments

We thank Titia de Lange (Rockefeller University, New York) for advice and provision of overexpression vectors for TRF1, TRF2, and RAP1; Ian Hickson for providing the anti-RAD51D antibody IH42; and Nasser Hajibagheri for advice with the electron microscopy. We thank Jean-Yves Masson for his assistance in the early stages of these studies; Julia Cooper and Alain Verreault for comments on the manuscript; and the members of our laboratory for their suggestions. This work was supported by Cancer Research UK (S.C.W.); the Swiss Bridge Fund (S.C.W. and M.A.B.); the Breast Cancer Campaign (S.C.W.); the Spanish Ministry of Science and Technology, the Regional Government of Madrid, the European Union, the Josef Steiner Foundation, and the Spanish National Cancer Center (M.A.B.); and the American Cancer Society and the March of Dimes Birth Defects Foundation (D.L.P.). M.T. and A.C. were supported in part by postdoctoral fellowships from EMBO and by the Dr. Mildred Scheel Cancer Foundation, respectively. P.M. is a Ramón y Cajal Senior Scientist.

Received: December 15, 2003
Revised: March 2, 2004
Accepted: March 8, 2004
Published: April 29, 2004

References

Bailey, S.M., Meyne, J., Chen, D.J., Kurimasa, A., Li, G.C., Lehnert, B.E., and Goodwin, E.H. (1999). DNA double-strand break repair proteins are required to cap the ends of mammalian chromosomes. Proc. Natl. Acad. Sci. USA *96*, 14899–14904.

Barlow, A.L., Benson, F.E., West, S.C., and Hultén, M.A. (1997). Distribution of RAD51 recombinase in human and mouse spermatocytes. EMBO J. *16*, 5207–5215.

Baumann, P., and Cech, T.R. (2001). Pot1, the putative telomere end-binding protein in fission yeast and humans. Science *292*, 1171–1175.

Baumann, P., Podell, E., and Cech, T.R. (2002). Human POT1 (protection of telomeres) protein: cytolocalization, gene structure, and alternative splicing. Mol. Cell. Biol. *22*, 8079–8087.

Bianchi, A., and de Lange, T. (1999). Ku binds telomeric DNA *in vitro*. J. Biol. Chem. *274*, 21223–21227.

Blackburn, E.H. (2001). Switching and signaling at the telomere. Cell *106*, 661–673.

Blasco, M.A., Lee, H.W., Hande, P.M., Samper, E., Lansdorp, P.M., DePinho, R.A., and Greider, C.W. (1997). Telomere shortening and tumor formation by mouse cells lacking telomerase RNA. Cell *91*, 25–34.

Braybrooke, J.P., Spink, K.G., Thacker, J., and Hickson, I.D. (2000). The RAD51 family member, RAD51L3, is a DNA-stimulated ATPase that forms a complex with XRCC2. J. Biol. Chem. *275*, 29100–29106.

Braybrooke, J.P., Li, J.-L., Wu, L., Caple, F., Benson, F.E., and Hickson, I.D. (2003). Functional interaction between the Bloom's syndrome helicase and the RAD51 paralog, RAD51L3 (RAD51D). J. Biol. Chem. *278*, 48357–48366.

Brummelkamp, T.R., Bernards, R., and Agami, R. (2002). A system for stable expression of short interfering RNAs in mammalian cells. Science *296*, 550–553.

Bryan, T.M., Englezou, A., Gupta, J., Bacchetti, S., and Reddel, R.R. (1995). Telomere elongation in immortal human cells without detectable telomerase activity. EMBO J. *14*, 4240–4248.

Chong, L., van Steensel, B., Broccoli, D., Erdjument-Bromage, H., Hanish, J., Tempst, P., and de Lange, T. (1995). A human telomeric protein. Science *270*, 1663–1667.

Colgin, L.M., Baran, K., Baumann, P., Cech, T.R., and Reddel, R.R. (2003). Human POT1 facilitates telomere elongation by telomerase. Curr. Biol. *13*, 942–946.

Constantinou, A., Davies, A.A., and West, S.C. (2001). Branch migration and Holliday junction resolution catalyzed by activities from mammalian cells. Cell *104*, 259–268.

D'Andrea, A.D., and Grompe, M. (2003). The Fanconi anaemia BRCA pathway. Nat. Rev. Cancer *3*, 23–34.

Davies, A.A., Masson, J.-Y., McIlwraith, M.J., Stasiak, A.Z., Stasiak, A., Venkitaraman, A.R., and West, S.C. (2001). Role of BRCA2 in control of the RAD51 recombination and DNA repair protein. Mol. Cell *7*, 273–282.

de Lange, T. (2002). Protection of mammalian telomeres. Oncogene *21*, 532–540.

Dobson, M.J., Pearlman, R.E., Karaiskakis, A., Spyropoulos, B., and Moens, P.B. (1994). Synaptonemal complex proteins: occurrence, epitope mapping, and chromosome disjunction. J. Cell Sci. *107*, 2749–2760.

Dunham, M.A., Neumann, A.A., Fasching, C.L., and Reddel, R.R. (2000). Telomere maintenance by recombination in human cells. Nat. Genet. *26*, 447–450.

Espejel, S., Franco, S., Rodriguez-Perales, S., Bouffler, S.D., Cigudosa, J.C., and Blasco, M.A. (2002). Mammalian Ku86 mediates chromosomal fusions and apoptosis caused by critically short telomeres. EMBO J. *21*, 2207–2219.

Ferreira, M.G., Miller, K.M., and Cooper, J.P. (2004). Indecent exposure: when telomeres become uncapped. Mol. Cell *13*, 7–18.

German, J. (1993). Bloom syndrome: a mendelian prototype of somatic mutational disease. Medicine *72*, 393–406.

Gilley, D., Tanaka, H., Hande, M.P., Kurimasa, A., Li, G.C., Oshimura, M., and Chen, D.J. (2001). DNA-PK_{cs} is critical for telomere capping. Proc. Natl. Acad. Sci. USA *98*, 15084–15088.

Goytisolo, F.A., Samper, E., Edmonson, S., Taccioli, G.E., and

Blasco, M.A. (2001). The absence of the DNA-dependent protein kinase catalytic subunit in mice results in anaphase bridges and in increased telomeric fusions with normal telomere length and G-strand overhang. Mol. Cell. Biol. *21*, 3642–3651.

Griffith, J.D., Comeau, L., Rosenfield, S., Stansel, R.M., Bianchi, A., Moss, H., and de Lange, T. (1999). Mammalian telomeres end in a large duplex loop. Cell *97*, 503–514.

Harley, C.B., Futcher, A.B., and Grieder, C.W. (1990). Telomeres shorten during ageing of human fibroblasts. Nature *345*, 458–460.

Hemann, M.T., Strong, M.A., Hao, L.-Y., and Greider, C.W. (2001). The shortest telomere, not average telomere length, is critical for cell viability and chromosome stability. Cell *107*, 67–77.

Henson, J.D., Neumann, A.A., Yeager, T.R., and Reddel, R.R. (2002). Alternative lengthening of telomeres in mammalian cells. Oncogene *21*, 598–610.

Herrera, E., Samper, E., Martin-Caballero, J., Flores, J.M., Lee, H.-W., and Blasco, M.A. (1999). Disease states associated to telomere deficiency appear earlier in mice with short telomeres. EMBO J. *18*, 2950–2960.

Hsu, H.L., Gilley, D., Blackburn, E.H., and Chen, D.J. (1999). Ku is associated with the telomere in mammals. Proc. Natl. Acad. Sci. USA *96*, 12454–12458.

Hsu, H.L., Gilley, D., Galande, S.A., Hande, M.P., Allen, B., Kim, S.H., Li, G.C., Campisi, J., Kohwi-Shigematsu, T., and Chen, D.J. (2000). Ku acts in a unique way at the mammalian telomere to prevent end joining. Genes Dev. *14*, 2807–2812.

Jacks, T., Remington, L., Williams, B.O., Schmitt, B.M., Halachmi, S., Bronson, R.T., and Weinberg, R.A. (1994). Tumor spectrum analysis in p53-mutant mice. Curr. Biol. *4*, 1–7.

Jaco, I., Muñoz, P., Goytisolo, F., Wesoly, J., Bailey, S., Taccioli, G., and Blasco, M.A. (2003). Role of mammalian RAD54 in telomere length maintenance. Mol. Cell. Biol. *23*, 5572–5580.

Karlseder, J., Broccoli, D., Dai, Y., Hardy, S., and de Lange, T. (1999). p53- and ATM-dependent apoptosis induced by telomeres lacking TRF2. Science *283*, 1321–1325.

Khanna, K.K., and Jackson, S.P. (2001). DNA double-strand breaks: signalling, repair and the cancer connection. Nat. Genet. *27*, 247–254.

Kim, N.W., Piatyszek, M.A., Prowse, K.R., Harley, C.B., West, M.D., Ho, P.L., Coviello, G.M., Wright, W.E., Weinrich, S.L., and Shay, J.W. (1994). Specific association of human telomerase activity with immortal cells and cancer. Science *266*, 2011–2015.

Le, S., Moore, J.K., Haber, J.E., and Greider, C.W. (1999). RAD50 and RAD51 define two pathways that collaborate to maintain telomeres in the absence of telomerase. Genetics *152*, 143–152.

Liu, Y., Masson, J.-Y., Shah, R., O'Regan, P., and West, S.C. (2004). RAD51C is required for Holliday junction processing in mammalian cells. Science *303*, 243–246.

Loayza, D., and de Lange, T. (2003). POT1 as a terminal transducer of TRF1 telomere length control. Nature *423*, 1013–1018.

Lundblad, V. (2002). Telomere maintenance without telomerase. Oncogene *21*, 522–531.

Maser, R.S., and DePinho, R.A. (2002). Connecting chromosomes, crisis, and cancer. Science *297*, 565–569.

Masson, J.-Y., Tarsounas, M.C., Stasiak, A.Z., Stasiak, A., Shah, R., McIlwraith, M.J., Benson, F.E., and West, S.C. (2001). Identification and purification of two distinct complexes containing the five RAD51 paralogs. Genes Dev. *15*, 3296–3307.

McEachern, M.J., Krauskopf, A., and Blackburn, E.H. (2000). Telomeres and their control. Annu. Rev. Genet. *34*, 331–358.

Moens, P.B., Chen, D.J., Shen, Z.Y., Kolas, N., Tarsounas, M., Heng, H.H., and Spyropolos, B. (1997). RAD51 immunocytology in rat and mouse spermatocytes and oocytes. Chromosoma *106*, 207–215.

Muñoz-Jordan, J.L., Cross, G.A., de Lange, T., and Griffith, J.D. (2001). T-loops at trypanosome telomeres. EMBO J. *20*, 579–588.

Opresko, P.L., von Kobbe, C., Laine, J.P., Harrigan, J., Hickson, I.D., and Bohr, V.A. (2002). Telomere-binding protein TRF2 binds to and stimulates the Werner and Bloom syndrome helicases. J. Biol. Chem. *277*, 41110–41119.

Pittman, D.L., and Schimenti, J.C. (2000). Mid-gestation lethality in mice deficient for the *recA*-related gene, Rad51d/Rad51L3. Genesis *26*, 167–173.

Ramirez, R., Carracedo, J., Jimenez, R., Canela, A., Herrera, E., Aljama, P., and Blasco, M.A. (2003). Massive telomere loss is an early event of DNA damage-induced apoptosis. J. Biol. Chem. *278*, 836–842.

Samper, E., Goytisolo, F., Slijepcevic, P., van Buul, P., and Blasco, M.A. (2000). Mammalian Ku86 protein prevents telomeric fusions independently of the length of TTAGGG repeats and the G-strand overhang. EMBO Rep. *1*, 244–252.

Scherthan, H., Jerratch, M., Li, B.M., Smith, S., Hultén, M., Lock, T., and de Lange, T. (2000). Mammalian meiotic telomeres: protein composition and redistribution in relation to nuclear pores. Mol. Biol. Cell *11*, 4189–4203.

Scully, R., Chen, J., Plug, A., Xiao, Y., Weaver, D., Feunteun, J., Ashley, T., and Livingston, D.M. (1997). Association of BRCA1 with RAD51 in mitotic and meiotic cells. Cell *88*, 265–275.

Stansel, R.M., de Lange, T., and Griffith, J.D. (2001). T-loop assembly *in vitro* involves binding of TRF2 near the 3' telomeric overhang. EMBO J. *20*, 5532–5540.

Stavropoulos, D.J., Bradshaw, P.S., Li, X., Pasic, I., Truong, K., Ikura, M., Ungrin, M., and Meyn, M.S. (2002). The Bloom syndrome helicase BLM interacts with TRF2 in ALT cells and promotes telomeric DNA synthesis. Hum. Mol. Genet. *11*, 3135–3144.

Takata, M., Sasaki, M.S., Tachiiri, S., Fukushima, T., Sonoda, E., Schild, D., Thompson, L.H., and Takeda, S. (2001). Chromosome instability and defective recombinational repair in knockout mutants of the five RAD51 paralogs. Mol. Cell. Biol. *21*, 2858–2866.

Tarsounas, M., Pearlman, R.E., and Moens, P.B. (1999). Meiotic activation of rat pachytene spermatocytes with okadaic acid: the behavior of synaptonemal complex components SYN1/SCP1 and COR1/SCP3. J. Cell Sci. *112*, 423–434.

Tarsounas, M., Davies, D., and West, S.C. (2003). BRCA2-dependent and independent formation of RAD51 nuclear foci. Oncogene *22*, 1115–1123.

Teng, S.C., and Zakian, V.A. (1999). Telomere-telomere recombination is an efficient bypass pathway for telomere maintenance in *Saccharomyces cerevisiae*. Mol. Cell. Biol. *19*, 8083–8093.

Thacker, J. (1999). A surfeit of *RAD51*-like genes? Trends Genet. *15*, 166–168.

Tong, W.-M., Hande, M.P., Lansdorp, P.M., and Wang, Z.-Q. (2001). DNA strand break-sensing molecule poly(ADP-ribose) polymerase cooperates with p53 in telomere function, chromosome stability, and tumor suppression. Mol. Cell. Biol. *21*, 4046–4054.

van Steensel, B., Smogorzewska, A., and de Lange, T. (1998). TRF2 protects human telomeres from end-to-end fusions. Cell *92*, 401–413.

Venkitaraman, A.R. (2002). Cancer susceptibility and the functions of BRCA1 and BRCA2. Cell *108*, 171–182.

Yokoyama, H., Kurumizaka, H., Ikawa, S., Yokoyama, S., and Shibata, T. (2003). Holliday junction binding activity of the human RAD51B protein. J. Biol. Chem. *278*, 2767–2772.

Zhu, X.D., Kuster, B., Mann, M., Petrini, J.H., and de Lange, T. (2000). Cell-cycle-regulated association of RAD50/MRE11/NBS1 with TRF2 and human telomeres. Nat. Genet. *25*, 347–352.

Zhu, X.D., Nierdernhofer, L., Kuster, B., Mann, M., Hoeijmakers, J.H., and de Lange, T. (2003). ERCC1/XPF removes the 3′ overhang from uncapped telomeres and represses formation of telomeric DNA containing double minute chromosomes. Mol. Cell *12*, 1489–1498.